Unveiling the Synthesis, Spectral Characterizations, and Electrochemical Potential of Novel (E)-Furan-2-yl Acrylohydrazides: An Exploration in Molecular Design

Penayori Marie-Aimée Coulibaly,[1] Souleymane Coulibaly,[1*] Sieny Roger N'Dri,[2] Evrard Ablo,[1,3] Amian Brise Kassi,[1] Drissa Sissouma,[1] and Adjou Ané[1]

[1]Laboratoire de Constitution et Réaction de la Matière, UFR Sciences des Structures de la Matière et Technologie, Université Felix Houphouët Boigny, 22 BP 582 Abidjan 22, Côte d'Ivoire

[2]Laboratoire des sciences physiques fondamentales et appliquées, École Normale Supérieure 08 BP 10 Abidjan, Côte d'Ivoire.

[3]Laboratoire des Procédés Industriels de Synthèse, de l'Environnement et des Énergies Nouvelles (LAPISEN), Institut National Polytechnique Félix Houphouët-Boigny, Yamoussoukro, Côte d'Ivoire

[*]Corresponding Author: souleymane.coulibaly87@ufhb.edu.ci; souleydestras@yahoo.fr
ORCID: https://orcid.org/0000-0003-4573-5978

Abstract

In this study, we present the synthesis of novel derivatives of 3-furan-2-yl acrylohydrazide using a meticulous three-step reaction sequence. The synthesis ends up in the condensation of (E)-3-(furan-2-yl) acrylohydrazine (**3**) with diverse benzaldehyde and acetophenone derivatives. Comprehensive characterization of the synthesized compounds was achieved through 1D NMR spectroscopic analyses (^{1}H and ^{13}C NMR), 2D NMR spectroscopy (HSQC, NOESY), and high-resolution mass spectrometry (HRMS).

The investigation of ^{1}H NMR data at room temperature in deuterated dimethyl sulfoxide (DMSO-d_6) unveiled the existence of (E)-3-(furan-2-yl) acrylohydrazide derivatives (**4a-h**) in a conformational equilibrium, manifesting as a mixture of synperiplanar E (sp E) and antiperiplanar E (ap E), or synperiplanar Z (sp Z) and antiperiplanar Z (ap Z). Notably, compounds **4a** and **4b** predominantly adopted the sp E conformer (Ec=c sp $E_{C=N}$), while compounds **4c** and **4d** favored the antiperiplanar conformation.

https://doi.org/10.26434/chemrxiv-2024-f8gtf **ORCID:** https://orcid.org/0000-0003-4573-5978 Content not peer-reviewed by ChemRxiv. **License:** CC BY 4.0

For the remaining compounds (**4e-h**), both conformers were nearly equimolar, with a marginal preference for the *anti* over the *syn* conformer. Interestingly, compounds **4f** and **4h** exhibited a prevalence of the apZ conformer (Ec=c ap $Z_{C=N}$), while compound **4e** featured the apE conformer (Ec=c ap $E_{C=N}$).

UV-visible absorption spectra for the N-acylhydrazones (**4a-h**) indicated absorption within the 570-635 nm range. Furthermore, cyclic voltammetry results demonstrated the capacity of the synthesized (E)-3-(furan-2-yl) acrylohydrazide derivatives (**4a-h**) to undergo quasi-reversible oxidation and reduction processes on a platinum electrode. These findings contribute valuable insights into the conformational dynamics and electrochemical behavior of this class of compounds, holding significance for applications in diverse scientific and technological domains.

Keywords**:** (E)-3-(furan-2-yl)acrylohydrazide, Acylhydrazone, Conformational analysis, Cyclic Voltammetry, UV-visible Absorption, NMR Spectroscopy.

Introduction

N-acylhydrazones (NAH) are distinguished by the presence of an azomethine fragment (CO–NH–N=CH), which, when integrated or connected into a heterocyclic scaffold, frequently yields compounds exhibiting noteworthy biological activities,[1-3] including anticancer,[4,5] antibacterial,[6] and antidepressant properties.[7] Acrylohydrazides, a distinct class within these organic compounds, have recently garnered attention due to their multifunctional properties.[8] Among them, (E)-3-(furan-2-yl) acrylohydrazides stand out, featuring the conjugated furan-2-yl scaffold linked to a hydrazide function. This unique combination of structures holds considerable potential for diverse applications, encompassing both bioactive functionalities and within the realm of optoelectronic conduction.[9]

The electronic conjugation intrinsic to these molecules can significantly influence charge transport properties, offering opportunities for exploitation in the development of optoelectronic devices such as organic light-emitting diodes (OLEDs),[10] and organic field-effect transistors (OFETs).[11]

Building upon our prior studies,[12,13] which consistently established the stable (E) conformation of N-acylhydrazones in various solvents, particularly the prevalence of the *syn* conformation in solvents like DMSO-d_6, we identified conditions favoring the *anti* conformation, including less polar solvents (e.g., $CDCl_3$), intramolecular hydrogen bonding, or steric hindrance. The persistent dominance of the *syn* conformation, where crucial

https://doi.org/10.26434/chemrxiv-2024-f8gtf **ORCID:** https://orcid.org/0000-0003-4573-5978 Content not peer-reviewed by ChemRxiv. **License:** CC BY 4.0

substituents adopt specific spatial orientations, suggests a structural regularity with promising implications for the design of novel molecules tailored for specific purposes.

Aligned with our previous investigations characterizing benzimidazoles N-acylhydrazones and acylhydrazones derived from nitroimidazo[1,2-a]pyridine, intimately linked to (E)-3-(furan-2-yl) acrylohydrazides by their fundamental structure, this study endeavors to comprehensively explore the preferential conformation of these newly synthesized molecular entities. Employing a rigorous synthetic approach coupled with structural analyses, encompassing NMR, HRMS, UV-visible, and cyclic voltammetry, our objective is to delve into the optoelectronic properties of (E)-3-(furan-2-yl) acrylohydrazides. Ultimately, this research aspires to make a significant contribution to the understanding of molecular conformation, thereby laying the foundation for potential applications in the field of materials science.

MATERIAL AND METHODS

I. Material

Unless otherwise stated, ^{1}H et ^{13}C NMR spectra were recorded at 500 and 126 MHz, at 400 MHz for ^{1}H and 101 MHz for ^{13}C, respectively, in $CDCl_3$, Methanol-d_3, and DMSO-d_6 solutions provided by Eurisotop, using TMS as an internal reference. Chemical shifts are reported in ppm on the δ scale. Multiplicities are denoted as s (singlet), d (doublet), dd (doublet of doublet), t (triplet), q (quartet), m (multiplet), and coupling constants (J) are reported in Hz. High-resolution mass spectra (HRMS) were acquired in electrospray ionization (ESI) mode using an LC-MSD TOF mass analyzer. UV-Visible spectra were obtained using the DR3900 spectrophotometer and processed with Origin Pro.

Reaction monitoring and compound purity were assessed by thin-layer chromatography (TLC) on silica gel plates (Merck Kisselgel $60F_{254nm}$, silica thickness 0.2 mm) revealed under UV-Vis light (λ=254 and 365 nm). Product purification was carried out using silica gel column chromatography (Kisselgel SI60, 40-63).

Solid compound melting points were determined using a Köpfler melting point apparatus with a temperature range of 44-266 °C. Cyclic voltammetry of the compounds was performed using a three-electrode electrochemical cell connected to a PALMSENS potentiostat (Ecochemie Netherlands) and linked to a computer via PSTRACE software for automated voltammogram plotting.

https://doi.org/10.26434/chemrxiv-2024-f8gtf **ORCID:** https://orcid.org/0000-0003-4573-5978 Content not peer-reviewed by ChemRxiv. **License:** CC BY 4.0

Reagents for various syntheses were purchased from Sigma Aldrich, Thermo Scientific chemicals, Chem Lab, and Fluorochem. Solvents were supplied by Polychimie Côte d'Ivoire.

II. Methods

II.1. *Synthesis Procedure for (E)-Ethyl 3-(furan-2-yl)acrylate (2)*

In a 50 mL round-bottom flask (rbf) fitted with a magnetic stirrer, a reaction mixture comprising triphenylphosphine (PPh_3, 1.5 eq., 15.00 mmol), a saturated solution of sodium bicarbonate ($NaHCO_3$) (10 mL), ethyl 2-chloroacetate (1.5 eq, 15.00 mmol), and furan-2-carbaldehyde (1 eq, 10.00 mmol) was stirred at ambient temperature for a duration of 24 h. The reaction was monitored using thin-layer chromatography (TLC), and the completion of the reaction is indicated by TLC analysis. At the end of the reaction, the reaction mixture was extracted with dichloromethane (DCM), and the resulting organic layer was dried using magnesium sulfate (MgSO4) before undergoing concentration under reduced pressure. Subsequently, diethyl ether (Et_2O) was introduced to induce the precipitation of triphenylphosphine oxide ($O=PPh_3$), which was subsequently separated *via* filtration. The obtained crude product undergoes purification via column chromatography on silica gel, using cyclohexane or hexane as the eluent, resulting in the isolation of a brown oil with a purity of 98%.

***(E)-Ethyl-3-(furan -2-yl) acrylate (2)*; brown oil, yield = 98%**

^{1}H NMR (500 MHz, $CDCl_3$) δ 7.47 (d, *J* = 0.6 Hz, 1HAr), 7.42 (d, *J* = 15.7 Hz, 1H, CH=), 6.59 (d, *J* = 3.3 Hz, 1HAr), 6.45 (dt, *J* = 3.2, 1.6 Hz, 1HAr), 6.31 (d, *J* = 15.7 Hz, 1H, =CH), 4.27 – 4.19 (q, 2H, -CH_2-), 1.31 (t, *J* = 7.1, 1.3 Hz, 3H, -CH_3).

^{13}C NMR (126 MHz, $CDCl_3$) δ 167.02, 151.00, 144.69, 130.96, 116.01, 114.59, 112.25, 60.42, 14.32.

II.2 *Synthesis Procedure for (E)-3-(furan-2-yl) acrylohydrazide*

In a 50 mL rbf equipped with a magnetic stirrer, 1 g (1 eq, 6.00 mmol) of (E)-ethyl-3-(thiophen-2-yl) acrylate was dissolved in 2 mL of ethanol, followed by the addition of 1.5 mL (5 eq, 30.00 mmol) of hydrazine monohydrate (H_2N-NH_2.H_2O). The mixture was stirred for 3 h at room temperature. TLC, indicative of reaction completion, was performed. Upon cessation of the reaction, the reaction medium was extracted using DCM. The organic layer was washed multiple times with water (H_2O), then dried with $MgSO_4$ and concentrated under

https://doi.org/10.26434/chemrxiv-2024-f8gtf **ORCID:** https://orcid.org/0000-0003-4573-5978 Content not peer-reviewed by ChemRxiv. **License:** CC BY 4.0

reduced pressure. The crude product was purified by column chromatography on silica gel, using cyclohexane/ethyl acetate 80/20 as the eluent, yielding a beige powder (52%).

***(E)-3-(furan-2-yl) acrylohydrazide (3)*, beige powder, yield=52%, m.p= 72-74°C**

^{1}H NMR (500 MHz, $CDCl_3$) δ 7.46 – 7.42 (m, 2H), 7.19 (s, 1H, NH), 6.55 (d, *J* = 3.4 Hz, 1H, HAr), 6.45 – 6.43 (m, 1H, HAr), 6.27 (d, *J* = 15.3 Hz, 1H, =CH), 4.05 (s, 2H, NH_2).

^{13}C NMR (126 MHz, $CDCl_3$) δ 167.16, 151.23, 144.31, 128.60, 115.69, 114.33, 112.33.

II.3 *General Procedure for the Synthesis of Hydrazide-Hydrazone derivatives (4a-h)*

In a 10 mL schlenk equipped with a magnetic stirrer, a mixture was prepared by combining 0.21 mmol (1 eq) of 3-(furan-2-yl) acrylohydrazide, 0.23 mmol (1.1 eq) of fluoroacetophenone, 1.5 mL of ethanol, and 2 drops of concentrated hydrochloric acid (HCl). The resulting mixture was stirred at room temperature (r.t) for 3 h. Subsequently, the reaction medium was concentrated under reduced pressure and subjected to purification *via* silica gel chromatography, using a DCM/MeOH mixture (95/5) as eluent. The isolated product was obtained from this process.

***(2E, N'E) -N'-(1-(3-fluorophenyl) ethylidene) -3-(furan-2-yl) acrylohydrazide (4a),* gold yellow powder, yield=54%, m.p=172-174°C**

^{1}H NMR (500 MHz, Methanol-d_3) δ 7.74 (ddd, *J* = 10.9, 2.6, 1.7 Hz, 1H), 7.72 – 7.66 (m, 1H), 7.62 (d, *J* = 1.8 Hz, 1H), 7.55 (d, *J* = 15.4 Hz, 1H, -CH=CH-), 7.40 (td, *J* = 8.1, 5.9 Hz, 1H), 7.16 – 7.10 (m, 1H), 6.80 – 6.76 (m, 1H, -C=CH-), 6.75 (d, *J* = 3.4 Hz, 1H), 6.55 (dd, *J* = 3.5, 1.8 Hz, 1H), 2.30_{sp},2.36_{ap} (s, 3H).

^{13}C NMR (126 MHz, Methanol-d_3) δ 168.38sp, 164.43ap, 162.95sp, 162,9ap (d, J= 244,4 Hz, F-C=C), 152.45, 151.62, 151.44, 145.01, 144.78, 129.91, 129.84, 129.72, 129.66, 129.63, 129.04, 122.42, 121.82, 116.01, 115.94, 115.84, 115.67, 115.50, 114.87, 114.50, 113.84, 113.22, 113.03, 112.48, 112.28, 112.08, 12.90, 12.08.

^{1}H NMR (400 MHz, DMSO-d_6) δ 10.74ap, 10.69sp (s, 1H, NH), 7.85 (d, *J* = 13.0 Hz, 2H), 7.69 – 7.55 (m, 4H), 7.53 – 7.44 (m, 3H), 7.39 (d, *J* = 16.3 Hz, 1H), 7.24 (td, *J* = 8.4, 2.7 Hz, 2H), 6.96 – 6.91 (m, 1H), 6.91 – 6.80 (m, 3H), 6.65 – 6.58 (m, 3H), 2.32sp ; 2.29ap (s, 3H, CH_3).

***(2E, N'E) -N'-(1-(4-fluorophenyl) ethylidene) -3-(furan-2-yl) acrylohydrazide (4b),* gold yellow powder, yield=41%, m.p=178-180°C**

https://doi.org/10.26434/chemrxiv-2024-f8gtf **ORCID:** https://orcid.org/0000-0003-4573-5978 Content not peer-reviewed by ChemRxiv. **License:** CC BY 4.0

^{1}H NMR (500 MHz, Methanol-*d*$_3$) δ 8.00$_{ap}$ – 7.92$_{ap}$, 7.88 $_{sp}$ (m, 2H), 7.65 $_{sp,}$ 7.63$_{ap}$ (d, *J* = 1.9 Hz, 1H), 7.55$_{ap,}$ 7.50$_{sp}$ (d, *J* = 15.4 Hz, 1H), 7.13$_{(sp+ap)}$ (q, *J* = 8.8 Hz, 2H), 6.80 – 6.72$_{(ap+sp)}$ (m, 2H), 6.56 $_{(sp+ap)}$ (dd, *J* = 3.4, 1.8 Hz, 1H), 2.37$_{ap}$, 2.30 $_{sp}$ (s, 3H).
^{13}C NMR (126 MHz, Methanol-*d*$_3$) δ 168.27$_{sp}$, 164.28$_{ap}$ (C=O), 163.73$_{ap}$ (d, *J*=247,9Hz), 153.08 (CAr), 151.61$_{sp}$, 151.41$_{ap}$ (CAr), 144.81$_{sp}$, 144.64$_{ap}$ (N=CH), 134.34, 129.43, 128.79, 128.69$_{ap,}$ 127.98$_{sp}$ (d,J=8.5 Hz), 116.00, 114.62$_{(sp+ap)}$ (d, *J* = 21.9 Hz), 114.24$_{ap}$, 113.95$_{sp}$, 111.96, 12.88$_{ap}$, 12.00$_{sp}$ (CH_3).

HMRS (ESI) : Calc. $C_{15}H_{14}N_2O_2F$ [M+H] =273.10393 found =273.10333.
Calc. $C_{15}H_{13}N_2O_2F$ [M-H] =271.08828 found =271.08953.

^{1}H NMR (500 MHz, DMSO-*d*$_6$) δ (ppm) 10.68 (s, 1H), 10.64 (s, 1H), 7.91 – 7.80 (m, 6H), 7.51 (d, *J* = 15.8 Hz, 1H), 7.43 (d, *J* = 15.5 Hz, 1H), 7.35 (d, *J* = 15.8 Hz, 1H), 7.28 (dt, *J* = 13.0, 8.8 Hz, 4H), 6.94 (d, *J* = 3.4 Hz, 1H), 6.88 – 6.81 (m, 3H), 6.64 (ddd, *J* = 7.9, 3.3, 1.7 Hz, 2H), 2.32sp, 2.29ap (s, 3H).
^{13}C NMR (126 MHz, DMSO-*d*$_6$) δ 166.70, 163.81, 161.94, 151.19, 150.55, 147.03, 145.54, 145.17, 134.79, 129.06, 128.62, 128.56, 128.24, 128.18, 127.50, 117.93, 115.41, 115.33, 115.16, 114.66, 114.46, 112.70, 112.63, 14.16, 13.88.

(2E, N'E)'-3-(furan-2-yl) -N'-(thiophen-2-ylmethylene) acrylohydrazide (4c), **Brown solid, yield=23%, m.p=216-218°C**
^{1}H NMR (500 MHz, DMSO-*d*$_6$) δ 11.60$_{ap}$, 11.48$_{sp}$ (s, 1H, NH), 8.46$_{ap}$, 8.24$_{sp}$ (s, 1H;N=CH), 7.89 – 7.81$_{(sp+ap)}$ (m, 1H), 7.65 (dd, *J* = 16.2, 5.0 Hz, 1H), 7.48 – 7.40$_{(sp+ap)}$ (m, 3H), 7.22$_{(sp+ap)}$ (d, *J* = 15.8 Hz, 1H), 7.14$_{(sp+ap)}$ (td, *J* = 5.3, 3.5 Hz, 2H), 6.94 – 6.85$_{(sp+ap)}$ (m, 2H), 6.64$_{(sp+ap)}$ (ddd, *J* = 9.4, 3.4, 1.8 Hz, 2H), 6.47 (d, *J* = 15.6 Hz, 1H).
^{13}C NMR (126 MHz, DMSO-*d*$_6$) δ 165.50$_{sp}$, 161.20$_{ap}$ (C=O), 151.03$_{sp}$, 150.87$_{ap}$ (C-O), 145.51$_{sp}$, 145.21$_{ap}$ (N=CH), 141.81$_{ap}$, 138.19$_{sp}$ (C_{Ar}) 139.11$_{ap}$, 138.94$_{sp}$ (C_{Ar}), 130.89$_{ap}$, 130.20$_{sp}$, 128.91$_{ap}$, 128.86$_{sp}$, 128.23$_{sp}$, 127.91$_{sp}$, 127.83$_{ap}$, 127.60$_{ap}$, 117.22$_{ap}$, 115.40$_{sp}$, 114.76$_{ap}$, 113.81$_{sp}$, 112.62$_{sp}$, 112.57$_{ap}$.

(2E, N'E)'-N'-((1H pyrrol-2-yl) methylene) -3-(furan-2-yl) acrylohydrazide (4d), **green powder**, **yield= 48%, m.p= 236-238°C**

https://doi.org/10.26434/chemrxiv-2024-f8gtf **ORCID:** https://orcid.org/0000-0003-4573-5978 Content not peer-reviewed by ChemRxiv. **License:** CC BY 4.0

^{1}H NMR (500 MHz, DMSO-*d*$_6$) δ 11.54 – 11.48 (m, 1H, NH), 11.45 (s, 1H), 11.33 (s, 1H), 11.17 (s, 1H), 8.08 (s, 1H), 7.89 (s, 1H), 7.85 – 7.82 (m, 1H), 7.81 (d, *J* = 1.8 Hz, 1H), 7.43 (d, *J* = 2.0 Hz, 1H), 7.39 (d, *J* = 15.5 Hz, 1H), 6.95 – 6.89 (m, 2H), 6.83 (d, *J* = 3.3 Hz, 1H), 6.63 (ddd, *J* = 16.9, 3.4, 1.8 Hz, 2H), 6.50 – 6.47 (m, 2H), 6.46 (s, 0H), 6.43 (p, *J* = 1.7 Hz, 1H), 6.16 – 6.10 (m, 2H).

^{13}C NMR (126 MHz, DMSO-*d*$_6$) δ 165.36, 160.76, 151.40, 151.00, 145.11, 144.99, 139.72, 136.09, 128.35, 127.11, 127.03, 126.94, 122.53, 121.86, 117.74, 115.12, 114.57, 114.27, 113.30, 112.59, 112.49, 109.26, 109.14.

(2E, N'E)'-3-(furan-2-yl) -N'-(furan-2-ylmethylene) acrylohydrazide (4e), **beige powder, yield= 56%, m.p= 224-226°C**

^{1}H NMR (500 MHz, DMSO-*d*$_6$) δ 11.60_{ap}, 11.44_{sp} (s, 1H, NH), 8.13_{ap}, 7.94_{sp} (s, 1H, N=CH), $7.87 – 7.82_{ap}$ (m, 3H), $7.49 – 7.40_{sp}$ (m, 2H), $7.25_{(ap)}$ (d, *J* = 15.8 Hz, 1H,=CH), 6.92_{sp} (t, *J* = 2.8 Hz, 2H), 6.88_{sp} (dd, *J* = 15.3, 3.4 Hz, 2H), 6.64_{ap} (ddt, *J* = 5.1, 3.4, 2.1 Hz, 4H), $6.46_{(ap)}$ (d, *J* = 15.5 Hz, 1H,CH=).

^{13}C NMR (126 MHz, DMSO-*d*$_6$) δ 165.69_{sp}, 161.28_{ap} (C=O), 151.06_{sp}, 150.86_{ap} (C-O), 149.42_{ap}, 149.18_{sp} (C-O), 145.45_{sp}, 145.22_{ap}(CH-O), 145.15_{ap}, 144.91_{sp}(CH-O), 136.43_{ap}, 133.15_{sp} (N=CH)), 128.81_{sp}, 127.67_{ap} (C_{Ar}), 117.18_{ap}, 115.33_{sp} (C_{Ar}), 114.76_{ap}, 113.96_{sp} (C_{Ar}), 113.53_{ap}, 113.37_{sp} (C_{Ar}), 112.61_{sp}, 112.53_{ap} (C_{Ar}), 112.19_{ap}, 112.07_{sp} (C_{Ar}).

(2E, N'E)'-3-(furan-2-yl) -N'-(pyridin-2-ylmethylene) acrylohydrazide (4f), **yellow powder, yield= 96%, m.p= 104-106°C**

^{1}H NMR (500 MHz, Methanol-*d*$_3$) δ 8.55 (q, *J* = 5.7 Hz, 1H), 8.27 (d, *J* = 8.0 Hz, 1H), 8.19 (s, 1H), 8.05 (t, *J* = 4.0 Hz, 1H), 7.88 (t, *J* = 7.8 Hz, 1H), 7.64 (d, *J* = 1.8 Hz, 1H), 7.58 (d, *J* = 15.4 Hz, 1H), 7.45 – 7.39 (m, 1H), 6.77 (d, *J* = 3.4 Hz, 1H), 6.57 (td, *J* = 4.1, 1.9 Hz, 1H), 6.52 (d, *J* = 15.4 Hz, 1H).

^{13}C NMR (126 MHz, Methanol-*d*$_3$) δ 169.30sp, 165.42ap (C=O), 154.39, 152.97, 152.53, 150.21, 150.11, 148.28, 146.34, 144.60, 144.40, 142.48, 142.31, 138.64, 138.54, 131.29, 130.89, 125.93, 125.67, 122.30, 121.90, 116.68, 116.29, 114.77, 113.51, 111.17.

HMRS (ESI) : Calc. $C_{13}H_{12}N_3O_2$ [M+H] =242.09295 found =242.09242.

Calc. $C_{13}H_{10}N_3O_2$ [M-H] =240.07730 found =240.07813.

^{1}H NMR (400 MHz, DMSO-*d*$_6$) δ 11.89ap (s, 1H), 11.73sp (s, 1H), 8.60 (dd, *J* = 4.1, 2.3 Hz, 2H), 8.23ap (s, 1H), 8.10sp (s, 1H), 7.99 – 7.82 (m, 6H), 7.49 (dd, *J* = 15.6, 13.9 Hz, 2H),

https://doi.org/10.26434/chemrxiv-2024-f8gtf **ORCID:** https://orcid.org/0000-0003-4573-5978 Content not peer-reviewed by ChemRxiv. **License:** CC BY 4.0

7.42 (ddd, *J* = 7.3, 4.9, 1.3 Hz, 2H), 7.33 (d, *J* = 15.8 Hz, 1H), 6.98 (d, *J* = 3.4 Hz, 1H), 6.90 (d, *J* = 3.4 Hz, 1H), 6.65 (ddd, *J* = 7.9, 3.4, 1.8 Hz, 2H), 6.48 (d, *J* = 15.5 Hz, 1H).

***(2E, N'E) -N'-(1-(4chloro-3-nitrobenzylidene) -3-(furan-2-yl) acrylohydrazide (4g)*, yellow powder**, **yield= 69%, m.p= 98-100°C**

^{1}H NMR (500 MHz, Methanol-*d*$_3$) δ 8.43 (d, *J* = 2.0 Hz, 1H,N=CH), 8.23_{sp}, 8.17_{ap} (s, 1H), 8.03_{ap}, 8.00_{sp} (dd, *J* = 8.4, 2.0 Hz, 1H), 7.74_{sp},7.71_{ap} (d, *J* = 8.4 Hz, 1H), 7.65 (d, *J* = 1.8 Hz, 1H), $7.57_{(ap+p)}$ (d, *J* = 15.3 Hz, 1H), 6.82_{sp}, 6.79_{ap} (d, *J* = 3.4 Hz, 1H), 6.58 (dd, *J* = 3.4, 1.8 Hz, 1H), 6.50 (d, *J* = 15.3 Hz, 1H).

^{13}C NMR (126 MHz, Methanol-*d*$_3$) δ 167.81_{sp}, 164.02_{ap} (C=O), 151.52_{sp}, 151.14_{ap}, 148.61, 145.09_{sp}, 145.04_{ap} (N=CH), 144.20, 141.03, 140.70, 134.88, 131.96_{sp}, 131.80_{ap}, 131.34_{ap}, 130.47_{sp}, 129.96_{sp}, 129.52_{ap}, 126.85_{ap}, 126.58_{sp}, 123.47_{ap}, 123.14_{sp}, 115.13_{ap}, 115.03_{sp}, 114.34, 113.10, 112.17_{ap}, 111.99_{sp}.

HMRS (ESI) Calc. $C_{14}H_{11}ClN_3O_4$ [M+H] = 320.04381 found= 320.04275

Calc. $C_{14}H_9ClN_3O_4$ [M-H] = 318.02815 found= 318.02845

^{1}H NMR (500 MHz, DMSO-*d*$_6$) δ 11.93 (s, 1H), 11.75 (s, 1H), 8.40 – 8.34 (m, 2H), 8.29 (s, 1H), 8.10 (s, 1H), 7.89 – 7.80 (m, 3H), 7.53 – 7.43 (m, 2H), 7.30 (d, *J* = 15.7 Hz, 1H), 6.97 (d, *J* = 3.3 Hz, 1H), 6.89 (d, *J* = 3.4 Hz, 1H), 6.51 (d, *J* = 15.5 Hz, 1H).

^{13}C NMR (126 MHz, DMSO-*d*$_6$) δ 166.09, 161.63, 151.03, 150.80, 148.05, 147.86, 145.61, 145.41, 143.16, 140.00, 135.04, 134.82, 132.15, 131.46, 130.98, 129.44, 128.24, 125.66, 125.29, 123.58, 123.37, 116.85, 115.56, 115.17, 113.63, 112.65.

***(2E, N'E) -N'-(3-(benzyloxy) benzylidene) -3-(furan-2-yl) acrylohydrazide (4h),* yellow powder**, **yield= 40%, m.p= 116-118°C**

^{1}H NMR (500 MHz, CDCl$_3$) δ 9.33 (s, 1H), 7.78 (s, 1H), 7.62 (d, *J* = 15.7 Hz, 1H), 7.55 – 7.43 (m, 4H), 7.40 (t, *J* = 7.3 Hz, 4H), 7.34 (td, *J* = 7.7, 2.8 Hz, 2H), 7.28 (d, *J* = 1.4 Hz, 1H), 7.03 (ddd, *J* = 8.2, 2.7, 1.1 Hz, 1H), 6.67 (d, *J* = 3.4 Hz, 1H), 6.52 – 6.44 (m, 1H), 5.15 (s, 2H).

^{13}C NMR (126 MHz, CDCl$_3$) δ 167.75, 159.08, 151.80, 144.58, 143.64, 136.80, 135.28, 130.15, 129.81, 128.68, 128.12, 127.64, 120.62, 116.98, 114.87, 114.21, 112.74, 112.33, 70.16. **HMRS (ESI)** Calc. $C_{21}H_{19}N_2O$ [M+H] =347,13957 found =347,13864

Calc. $C_{21}H_{17}N_2O$ [M-H] =345.12391 found =345.12466

https://doi.org/10.26434/chemrxiv-2024-f8gtf **ORCID:** https://orcid.org/0000-0003-4573-5978 Content not peer-reviewed by ChemRxiv. **License:** CC BY 4.0

^{1}H NMR (400 MHz, DMSO-d_6) δ 11.70 (s, 1H), 11.53 (s, 1H), 8.19 (s, 1H), 8.01 (s, 1H), 7.89 – 7.80 (m, 2H), 7.52 – 7.25 (m, 20H), 7.12 – 7.04 (m, 2H), 6.95 (s, 0H), 6.64 (ddd, *J* = 7.8, 3.4, 1.8 Hz, 2H), 6.50 (d, *J* = 15.6 Hz, 1H), 5.17 (d, *J* = 11.4 Hz, 4H).
^{13}C NMR (101 MHz, DMSO-d_6) δ 165.84, 161.34, 158.64, 158.61, 151.10, 150.86, 146.45, 145.48, 145.23, 142.98, 136.96, 136.90, 135.76, 135.57, 130.02, 129.93, 128.97, 128.45, 128.42, 127.85, 127.73, 127.68, 120.02, 119.50, 117.27, 116.81, 116.48, 115.27, 114.81, 114.06, 112.65, 112.59, 112.47, 69.27.

III. Results and Discussion

III. 1. Chemical Synthesis

The N-acylhydrazone derivatives (**4a-h**) were obtained through a three-step synthetic pathway starting from furan-2-carboxaldehyde (**1**). The initial step involved the addition of ethyl chloroacetate to aldehyde (**1**) in the presence of triphenylphosphine (PPh_3) under basic conditions, employing the Wittig reaction.[14] Consequently, the ester (**2**) was obtained with a yield of 98 %. Subsequently, the ester (**2**) reacted with hydrazine monohydrate (H_2N-$NH_2.H_2O$) in ethanol at room temperature to yield the corresponding hydrazide (**3**) with a yield of 52 %. Finally, a series of acrylohydrazide derivatives (**4a-h**) was synthesized with yields ranging from 23 % to 96 %. This was achieved by condensing hydrazide (**3**) with various derivatives of benzaldehyde and acetophenone in ethanol at room temperature for 3 hours, in the presence of a catalytic amount of concentrated hydrochloric acid (HCl) (**Scheme 1**). The newly synthesized compounds (**4a-h**) were fully characterized using various analytical methods, notably NMR, which revealed the presence of a dynamic equilibrium between two isomers for each compound in the N-acrylohydrazone series (**4a-h**). The results of this stereochemical study will be discussed in the following section.

III. 2. Spectral Analysis

The examination of the ^{1}H NMR spectrum for compound (**2**) elucidates the presence of two distinctive doublets. One is discerned at 6.24 ppm, indicative of the alpha (α) proton proximate to the carbonyl CO, while the other is observed at 7.78 ppm, corresponding to the beta (β) proton. The pronounced mesomeric attractive effect between the alkene and the carbonyl bonds results in notable deshielding of the beta (β) proton in the vicinity of the carbonyl. Furthermore, a quadruplet, integrating for two protons around 4.2 ppm, and a triplet, integrating for three protons at 1.3 ppm, are evident, corroborating the presence of the methyl

https://doi.org/10.26434/chemrxiv-2024-f8gtf **ORCID:** https://orcid.org/0000-0003-4573-5978 Content not peer-reviewed by ChemRxiv. **License:** CC BY 4.0

group of the ester function. Aromatic protons manifest between 7.05 ppm and 7.36 ppm. In the ^{13}C NMR spectrum, a discernible peak at 166.83 ppm confirms the presence of the carbonyl carbon.

The scrutiny of the ^{1}H NMR spectrum for compound (**3**) reveals the disappearance of signals attributed to the ethoxy group (OCH_2CH_3) and the emergence of broad singlets at 4.05 and 7.19 ppm. These singlets correspond to the NH protons of the NH_2 and C(O)-NH groups, respectively.

The ^{1}H NMR spectra of the ultimate compounds (**4a-h**), acquired in DMSO-d_6, exhibit a marked duplication of signals pertaining to three neighboring atom groups within the amide fragment: NH, N=CH or N=C(CH_3), and CH=CH(CO) (**Figure 1**). **Table 2** provides the chemical shift data for the duplicated proton signals of the amide function, as well as the azomethine (N=CH) and azoethylidine (N=C(CH_3)) fragments. Additionally, a systematic duplication of signals is discernible in the ^{13}C NMR spectra for all compounds (**4a-h**). **Table 3** compiles the chemical shift values for the duplicated carbons of the amide carbonyl function, and the N=CH and N=C(CH_3) fragments.

Comparison of the ^{1}H NMR spectra (**Figure 4**) for compound (**4h**) recorded in deuterated chloroform ($CDCl_3$) and deuterated dimethyl sulfoxide (DMSO-d_6) reveals the presence of two conformers characterized by the splitting of the NH function signal, one at 11.76 ppm and the other at 11.59 ppm in the DMSO-d_6 spectrum. In contrast, the $CDCl_3$ spectrum indicates a singular conformer with the NH function signal appearing at 9.33 ppm. Notably, the chemical shift of NH is reduced in the $CDCl_3$ spectrum compared to the DMSO-d_6 spectrum. This observation aligns with the findings reported by Palla et *al*.[15], suggesting that the marginal chemical shifts observed in the $CDCl_3$ spectra may be attributed to intramolecular hydrogen bonding.

Comparative analysis of the ^{1}H NMR spectra for compounds **4b** and **4g**, recorded in deuterated methanol (Methanol-d_3) and DMSO-d_6 (**Figures 2 and 4**) indicates signal duplication for various protons. However, the NH signal is absent in the spectrum recorded in Methanol-d_3, and the duplicated signals exhibit lower intensity compared to the ^{1}H NMR spectrum recorded in DMSO-d_6. The duplicated NH signals manifest at 11.74 ppm and 11.93 ppm for compound (**4g**) and 10.63 ppm and 10.67 ppm for compound (**4b**). The absence of the NH signal in the spectra recorded in Methanol-d_3 may be ascribed to proton exchange with deuterium from the solvent.

III.3 Stereochemical analysis of Acrylohydrazide derivatives (4a-h)

https://doi.org/10.26434/chemrxiv-2024-f8gtf **ORCID:** https://orcid.org/0000-0003-4573-5978 Content not peer-reviewed by ChemRxiv. **License:** CC BY 4.0

The duplication of characteristic signals for NH and N=CH groups observed in both ^{1}H and ^{13}C NMR spectra (**Table 2 and 4**) of the acrylohydrazides (compounds **4a-h**) indicates the presence of two distinct isomers. Considering the structure of acrylohydrazide, this signal duplication could be attributed to the geometric stereoisomerism (Z or E) of the azomethine (N=CH) or azoethylidine (N=C(CH_3)) fragment, or the ethylenic (CH=CH) group, or to a slow rotation around the N-N or N-C=O bond.

Concerning the geometric stereoisomerism of the ethylenic fragment in acrylohydrazides, they all exhibit the $E_{c=c}$ configuration confirmed by the coupling constant (*J*=15.30-15.80 Hz) of the ethylenic proton signals ranging between 6.46 ppm and 7.62 ppm.

Due to the assembly of amide and imine functionalities, acrylohydrazides can exist as stereoisomers with a C=N double bond (geometric configurations Z or E) and as syn/antiperiplanar conformers around the amide (C(O)-NH) bond. In the ^{1}H NMR spectra, the maximum intensity difference for compounds (**4a-h**) confirms that both conformers were obtained with different ratios (**Table 2**). These ratios were calculated using the following relationship:

$$Rsyn = \frac{\text{Isyn}}{\text{Isyn} + \text{Ianti}} \quad et\ Ranti = \frac{\text{Ianti}}{Isyn + Ianti}$$

In this equation, I represent the intensity of each signal in the ^{1}H NMR spectrum, and R denotes the ratio. Analysis of the various ratios among all possible conformers reveals that the synperiplanar (sp) conformer is predominant for compounds **4a-b**, while the antiperiplanar (ap) conformer is favored for compounds **4c-d**. For compounds **4e-h**, the *syn*/*anti*-periplanar conformers are nearly in equal proportions.

Palla et *al.*'s previous work[15] has demonstrated that the Z isomer of acrylohydrazides is characterized by a singlet around 14 ppm corresponding to the NH proton. The absence of a singlet (duplicated) around this chemical shift in our proton spectra (**Figure 1**) suggests the absence of the $Zc=_{N}$ isomer. However, the lack of correlation between the NH proton and the azomethine fragment in the NOESY spectrum of compounds **4h** and **4f** confirms the presence of the Z(C=N) isomer, contradicting Palla et *al.*'s findings.[15] Regarding compounds **4a-b** and **4e**, the emergence of a weak correlation between the NH proton and azomethine (N=CH) and azoethylidine (N=C(CH_3)) fragments in the NOESY spectrum (**Figure 2**) confirms the presence of the E(C=N) isomer. **Table 3** summarizes the calculated ratios relative to the duplicated NH signal. These results indicate that the *syn* conformer is predominant for compounds **4a-b** (thus, the stereochemistry Ec=c sp $E_{C=N}$), while for compounds **4c-h**, the

https://doi.org/10.26434/chemrxiv-2024-f8gtf **ORCID:** https://orcid.org/0000-0003-4573-5978 Content not peer-reviewed by ChemRxiv. **License:** CC BY 4.0

anti conformer is favored. It is noteworthy that the proportion of the *anti* conformer decreases in favor of the *syn* conformer when transitioning from compounds **4c-d** to **4g-h** and from **4g-h** to **4e-f**. This variation in the proportion between *syn*/*anti* conformers in compounds **4c-h** may be linked to the diverse aromatic aldehydes used for their synthesis, as well as potential interactions during characterization.

Comparing the ratios of different conformers between compounds **4c-h** and **4a-b** reveals a reversal of the *anti* conformer in favor of the *syn* conformer when transitioning from compounds **4c-h** to **4a-b**. This inversion of conformers could be explained by the bulkier nature of the azoethylidine fragment (N=C(CH_3)) compared to the azomethine fragment (N=CH).

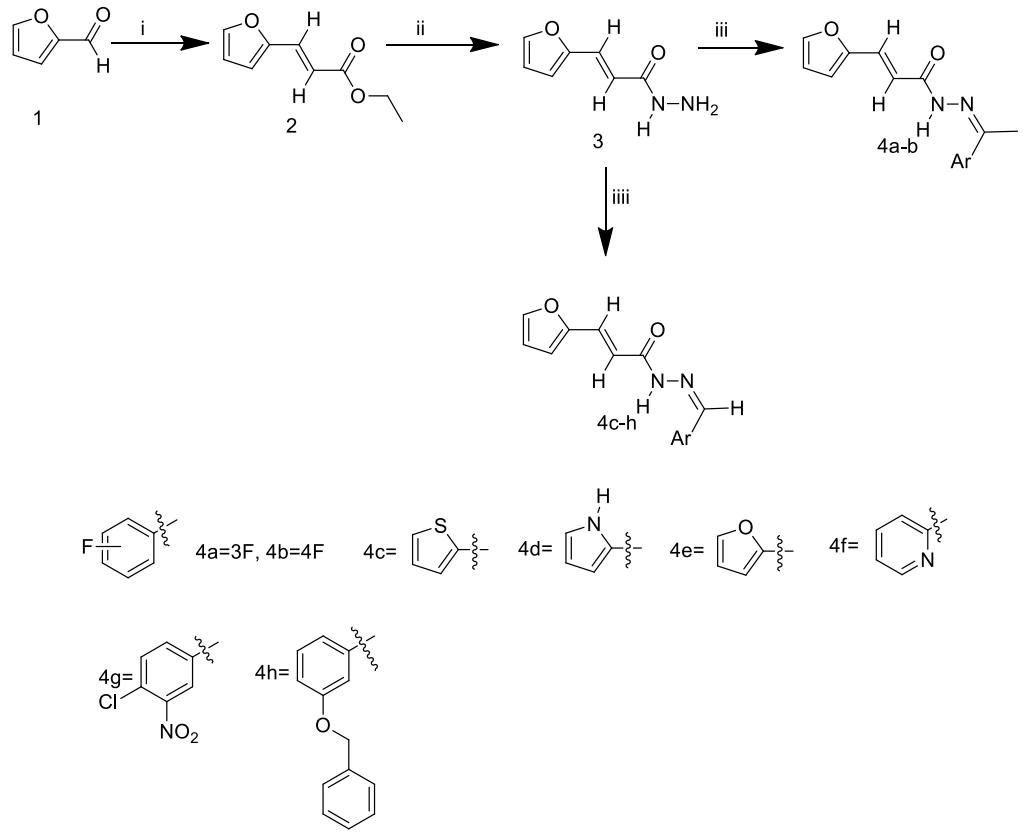

Scheme 1: Synthesis of acrylohydrazide derivatives
i. PPh_3, ethyl chloroacetate, $NaHCO_3$, ii. H_2NNH_2, EtOH, iii. EtOH, HCl, acetophenone derivatives, iv. EtOH, HCl, aldehydes.

https://doi.org/10.26434/chemrxiv-2024-f8gtf **ORCID:** https://orcid.org/0000-0003-4573-5978 Content not peer-reviewed by ChemRxiv. **License:** CC BY 4.0

Table1 : Acrylohydrazide derivatives obtained

Compounds	*Structure*	*Ar*	*Yield (%)*
4a	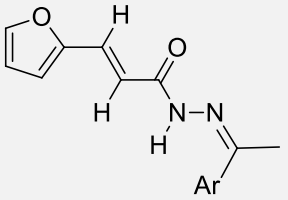	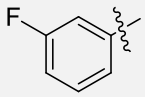	54
4b		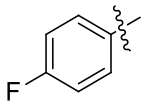	41
4c	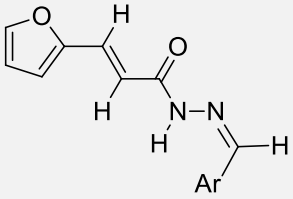	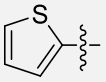	23
4d		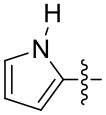	48
4e		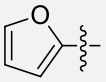	56
4f		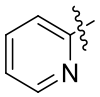	96
4g		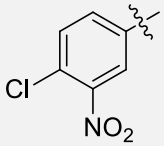	69
4h		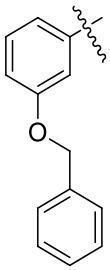	40

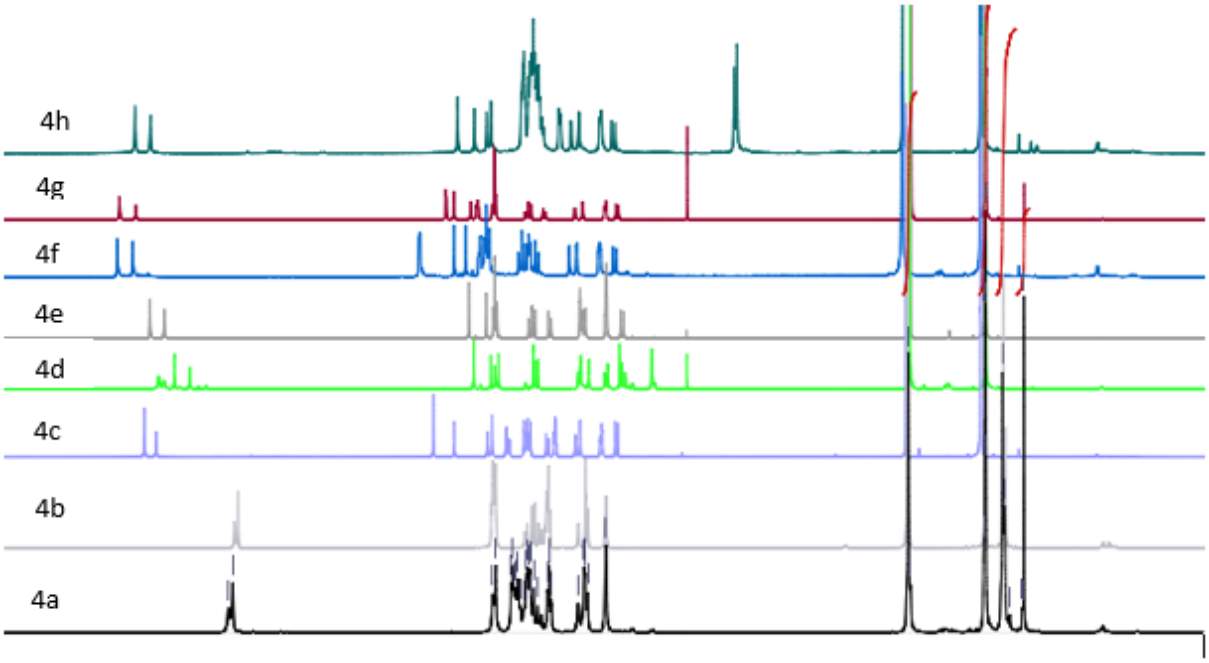

Figure 1: ^{1}H NMR spectra of compounds **4a-h**.

https://doi.org/10.26434/chemrxiv-2024-f8gtf **ORCID:** https://orcid.org/0000-0003-4573-5978 Content not peer-reviewed by ChemRxiv. **License:** CC BY 4.0

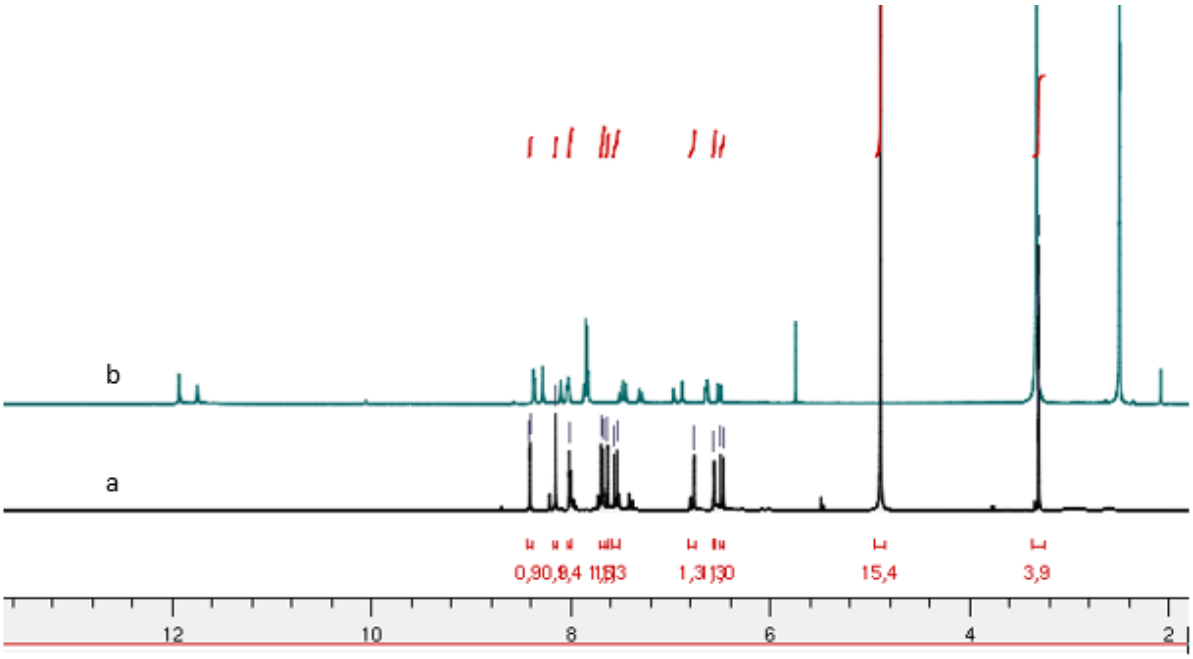

Figure 2: ^{1}H NMR spectrum of compound **4g**: (a) in Methanol-d_3 and (b) in DMSO-d_6

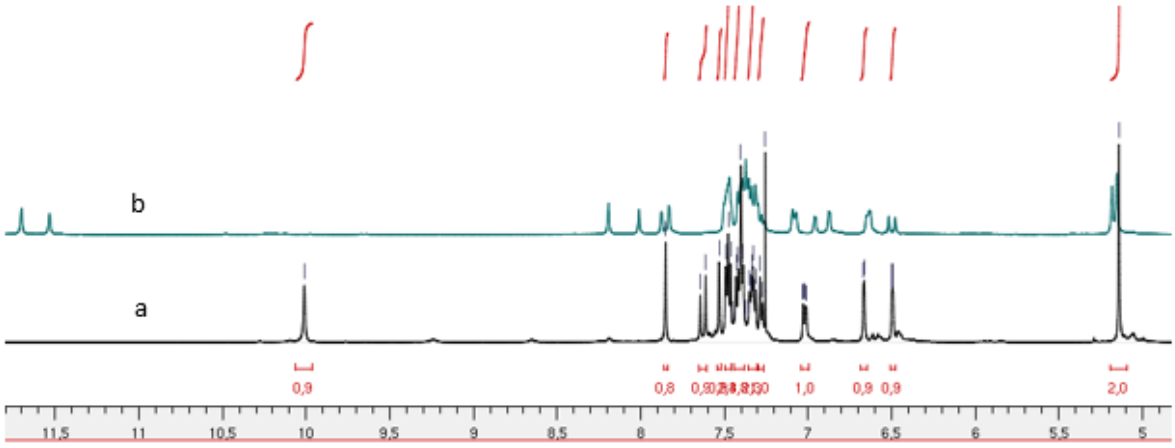

Figure 3: ^{1}H NMR spectrum of compound **4h**: (a) in $CDCl_3$ and (b) in DMSO-d_6

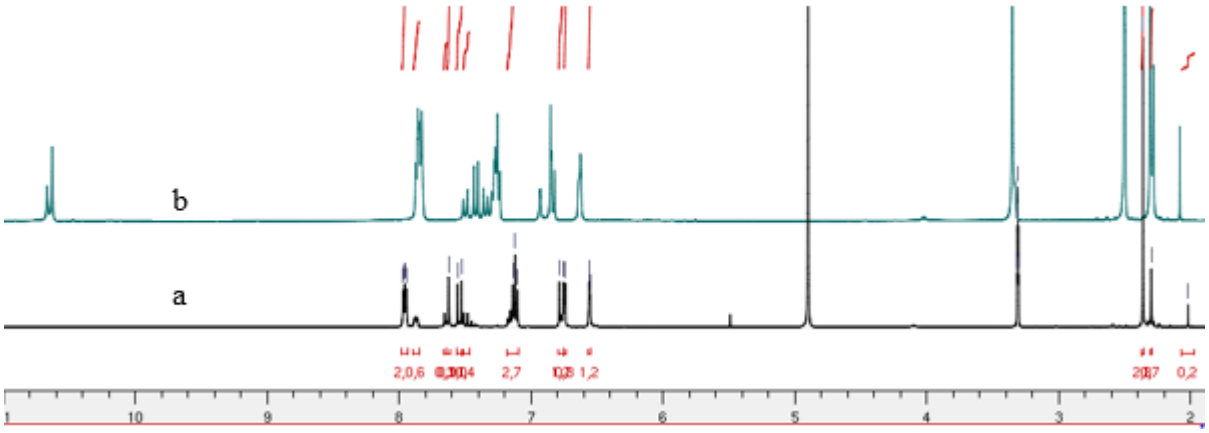

Figure 4: ^{1}H NMR spectrum of compound **4b**: (a) in methanol-d_3 et (b) in DMSO-d_6

https://doi.org/10.26434/chemrxiv-2024-f8gtf **ORCID:** https://orcid.org/0000-0003-4573-5978 Content not peer-reviewed by ChemRxiv. **License:** CC BY 4.0

Table 2: Chemical shift of protons in compounds **4a-h**

	Chemical shift δ (ppm)							*Yield*
	C(O)-NH		N=CH or N=C(CH_3)		Ar	Ratio (%)		(%)
Compounds	*anti*	*syn*	*anti*	*syn*		*anti*	*syn*	
4a	10.74	10.69	2.39	2.32	3-F-C_6H_4	38	62	42
4b	10.67	10.63	2.28	2.30	4-F- C_6H_4	38	62	41
4c	11.60	11.47	8.46	8.23	C_4H_3S	62	38	23
4d	11.33	11.16	8.07	7.88	C_4H_4N	62	38	48
4e	11.59	11.43	8.12	7.93	C_4H_3O	53	47	56
4f	11.89	11.72	8.22	8.10	C_5H_4N	53	47	96
4g	11.93	11.74	8.29	8.10	3-Cl-4-NO_2- C_6H_3	56	44	69
4h	11.76	11.59	8.25	8.06	3-O-CH_2-C_6H_5	56	44	69

Table 3: Proportion of ratios relative to C(O)-NH in compounds **4a-h**

Compounds	*Ratio (%) relative to C(O)-NH*		*Proportion*
	anti	*syn*	
4a	38	62	1 :1.6
4b	38	62	1 :1.6
4c	62	38	1.6 :1
4d	62	38	1.6 :1
4e	53	47	1.1 :1
4f	53	47	1.1 : 1
4g	56	44	1.3 :1
4h	56	44	1.3 :1

Table 4: Chemical shift of carbon in compounds **4a-h**

	Chemical shift δ ppm (^{13}C)				
	C(O)-NH		N=CH or N=C(CH_3)		Ar
Compounds	*anti*	*syn*	*anti*	*syn*	
4a	164.43	168.38	13.62	14.45	3-F-C_6H_4
4b	165.77	169.74	13.66	14.51	4-F- C_6H_4
4c	161.18	165.49	141.79	128.17	C_4H_3S
4d	160.75	165.36	139.72	136.09	C_4H_4N
4e	161.27	165.68	136.41	133.14	C_4H_3O
4f	165.42	169.30	-	-	C_5H_4N
4g	161.63	166.09	143.16	140.00	3-Cl-4-NO_2- C_6H_3

https://doi.org/10.26434/chemrxiv-2024-f8gtf **ORCID:** https://orcid.org/0000-0003-4573-5978 Content not peer-reviewed by ChemRxiv. **License:** CC BY 4.0

4h	161.39	165.84	-	-	3-O-CH_2-C_6H_5

Table 5: Stereoisomerism of the obtained compounds **(4a-h)**

Compounds	*Stereoisomerism*
4a	Ec=c sp $E_{C=N}$
4b	Ec=c sp $E_{C=N}$
4c	Ec=c ap -
4d	Ec=c ap -
4e	Ec=c ap $E_{C=N}$
4f	Ec=c ap $Z_{C=N}$
4g	Ec=c ap -
4h	Ec=c ap $Z_{C=N}$

(-) The geometric configuration of C=N could not be determined.

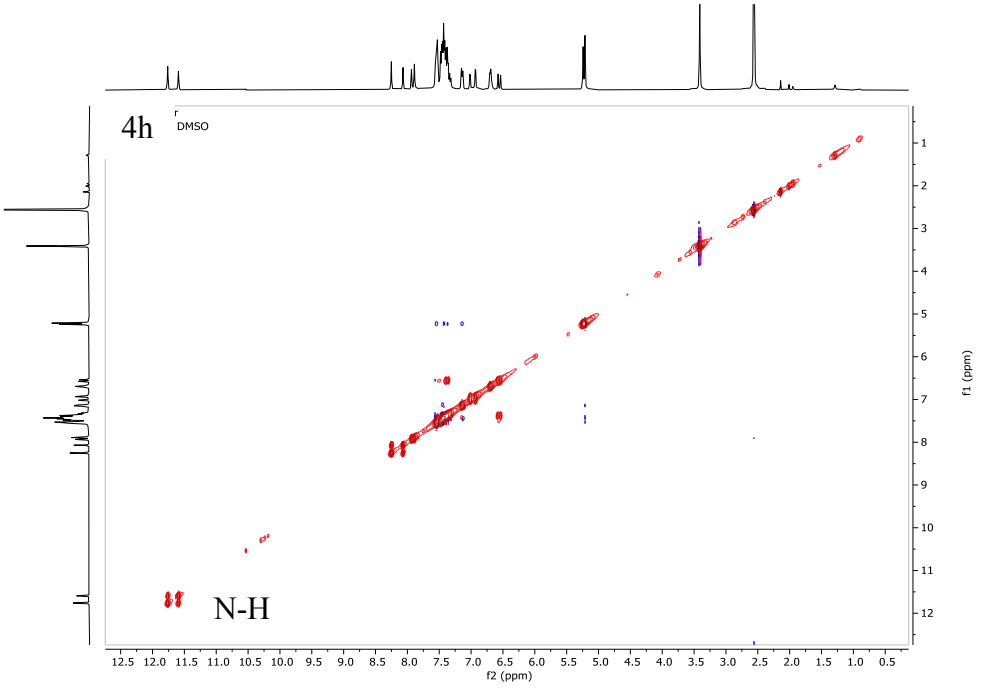

https://doi.org/10.26434/chemrxiv-2024-f8gtf **ORCID:** https://orcid.org/0000-0003-4573-5978 Content not peer-reviewed by ChemRxiv. **License:** CC BY 4.0

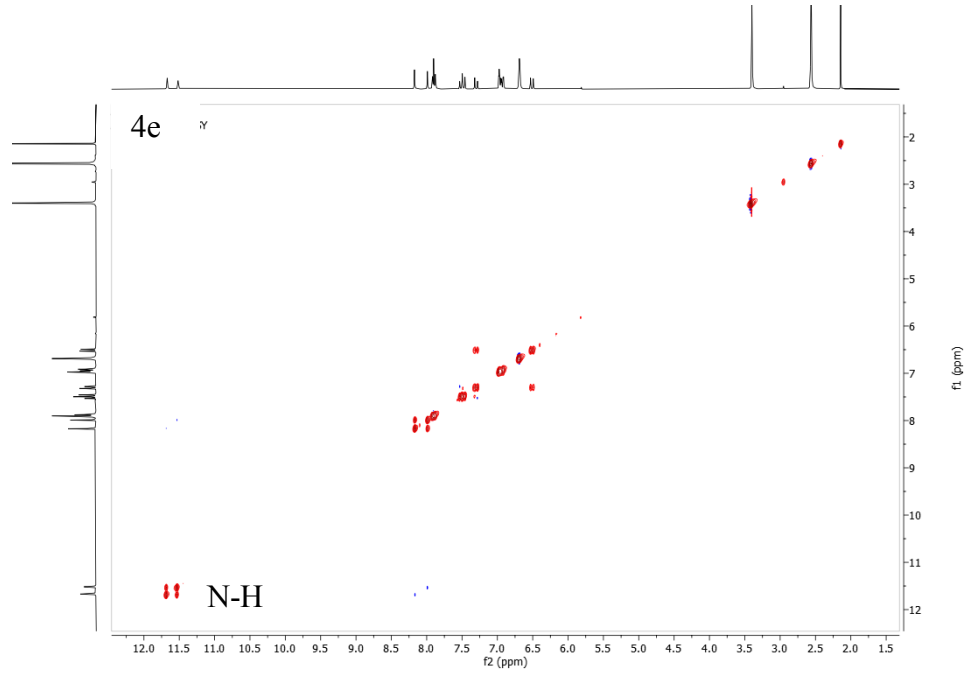

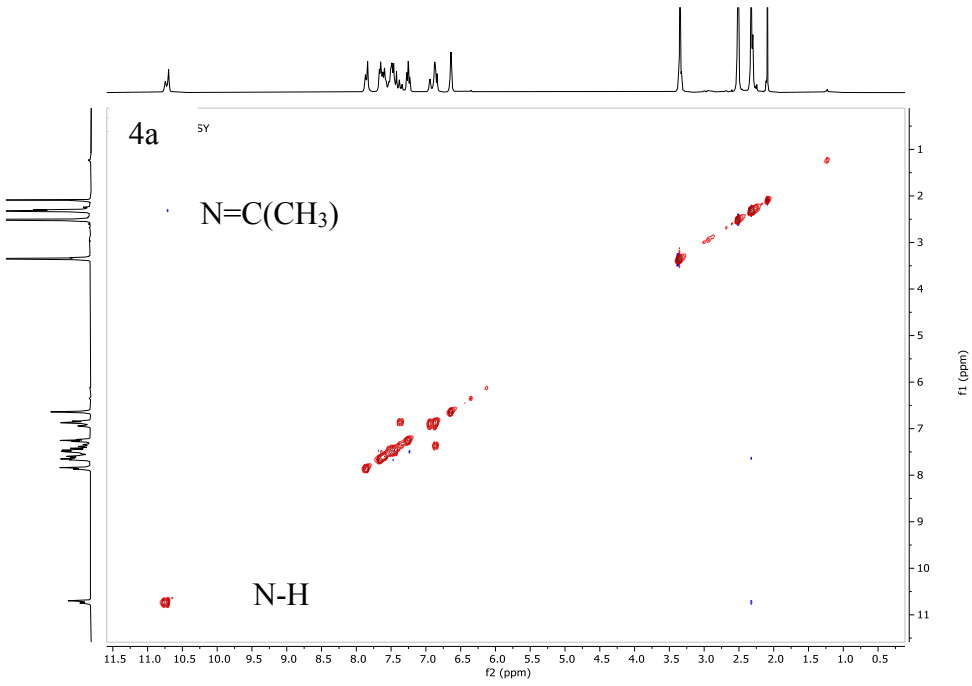

https://doi.org/10.26434/chemrxiv-2024-f8gtf **ORCID:** https://orcid.org/0000-0003-4573-5978 Content not peer-reviewed by ChemRxiv. **License:** CC BY 4.0

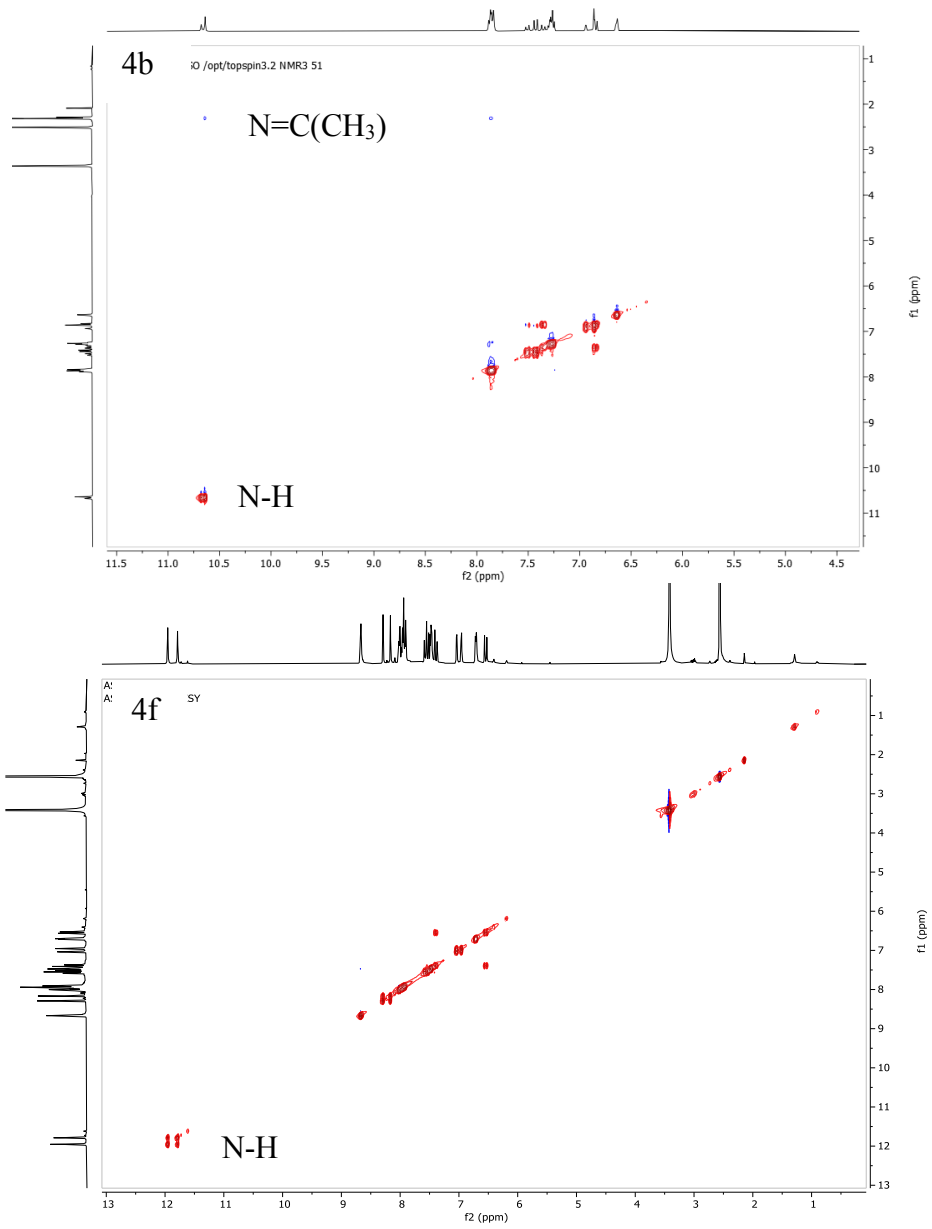

Figure 5: NOESY spectra in DMSO-d_6 of compounds **4a-b, 4e, 4f, 4h.**

https://doi.org/10.26434/chemrxiv-2024-f8gtf **ORCID:** https://orcid.org/0000-0003-4573-5978 Content not peer-reviewed by ChemRxiv. **License:** CC BY 4.0

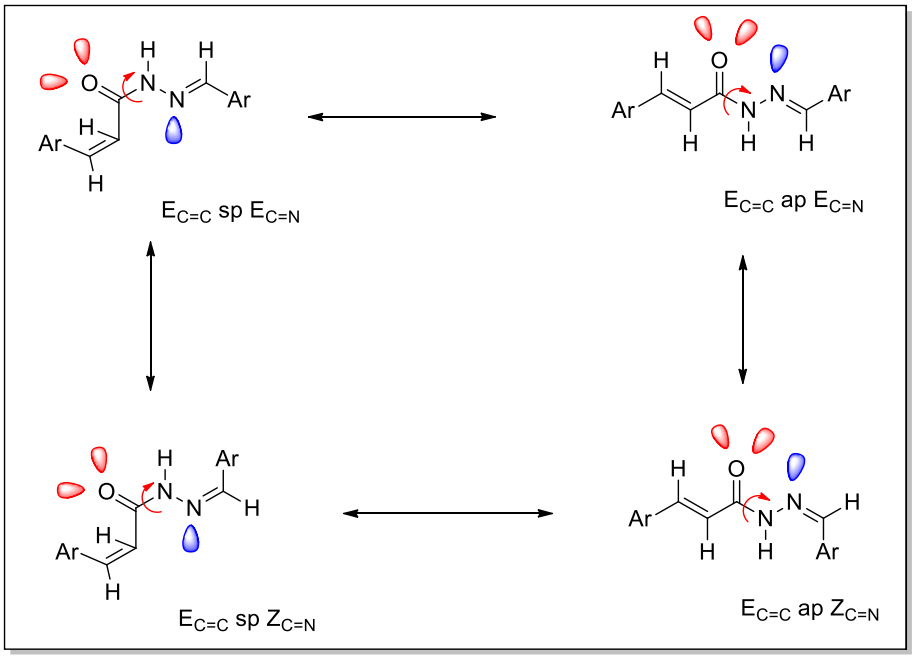

Scheme 2: The various possible conformers of the acrylohydrazides derivatives

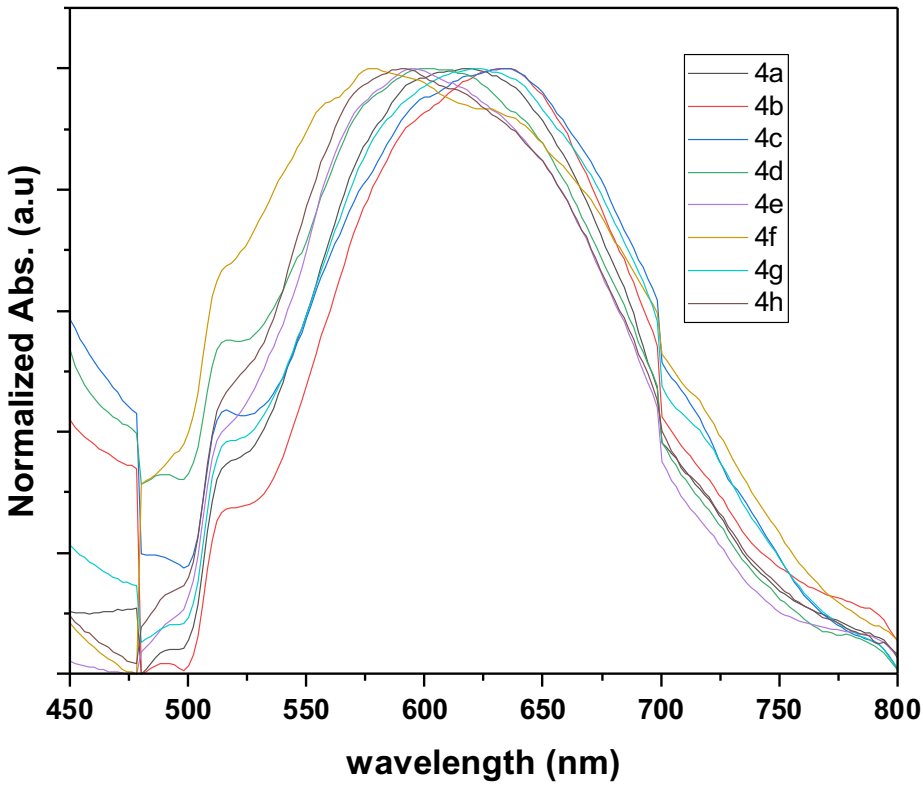

Figure 6: UV-visible absorption spectrum of compounds **4a-h** in DMSO at c=10^{-3} M

https://doi.org/10.26434/chemrxiv-2024-f8gtf **ORCID:** https://orcid.org/0000-0003-4573-5978 Content not peer-reviewed by ChemRxiv. **License:** CC BY 4.0

The graphical representation in **Figure 6** provides a comprehensive overview of the UV-visible absorption spectra for compounds **4a-h** dissolved in DMSO at a concentration of 10^{-3} M. Notably, all observed spectra exhibit a singular vibrational transition spanning the wavelength range of 475 to 800 nm, and the corresponding maximum absorption wavelengths are tabulated in **Table 6**.

The work of Li et *al.*[16] establishes a crucial framework for interpreting our results. Specifically, they demonstrated that absorption peaks falling within the range of 300 to 450 nm are indicative of π-π* electronic transitions, while those spanning 500 to 860 nm are attributed to intramolecular charge transfers. Leveraging these insights, we confidently affirm that the absorption features delineated in **Figure 6** for compounds 4a-h can be attributed to electronic vibrations associated with intramolecular charge transfers.

Remarkably, the absorption spectra of compounds **4a-h** exhibit congruent absorption bands with nearly identical intensities, underscoring the uniformity of their electronic transitions. However, a discernible bathochromic shift is evident in the absorption spectrum of compound **4b** relative to that of **4a.** This intriguing observation suggests a nuanced influence associated with the fluorine position. Further scrutiny of the absorption spectra of compounds **4c-d** reveals a bathochromic shift in the spectra of compounds **4c** and **4e** compared to that of **4d**. We posit that this spectral disparity is intricately linked to the distinct heteroatoms present within the cyclic structures of these compounds. Our meticulous analysis, informed by the contextualization of our findings within the existing literature, not only advances our understanding of the electronic properties of compounds **4a-h** but also underscores the potential impact of subtle structural modifications on their absorption characteristics. These insights bear significance not only for fundamental research in molecular electronics but also for the rational design of compounds with tailored electronic properties for specific applications.

Table 6: Values of the maximum absorption wavelengths for compounds **4a-h**

Compounds	λ_{max} ***(nm)***
4a	618
4b	633
4c	634
4d	600
4e	595
4f	578
4g	622
4h	591

https://doi.org/10.26434/chemrxiv-2024-f8gtf **ORCID:** https://orcid.org/0000-0003-4573-5978 Content not peer-reviewed by ChemRxiv. **License:** CC BY 4.0

The voltammograms of the studied compounds exhibit a consistent profile, featuring both oxidation and reduction peaks (**Figure 7**). The appearance of oxidation peaks (anodic peaks) in the voltammograms may be attributed to the oxidation of nitrogen atoms within the molecular structures. Conversely, the cathodic peak observed in the voltammograms is likely associated with the reduction of the ketone function (C=O). Acrylohydrazide derivatives undergo oxidation and reduction processes on the platinum electrode.

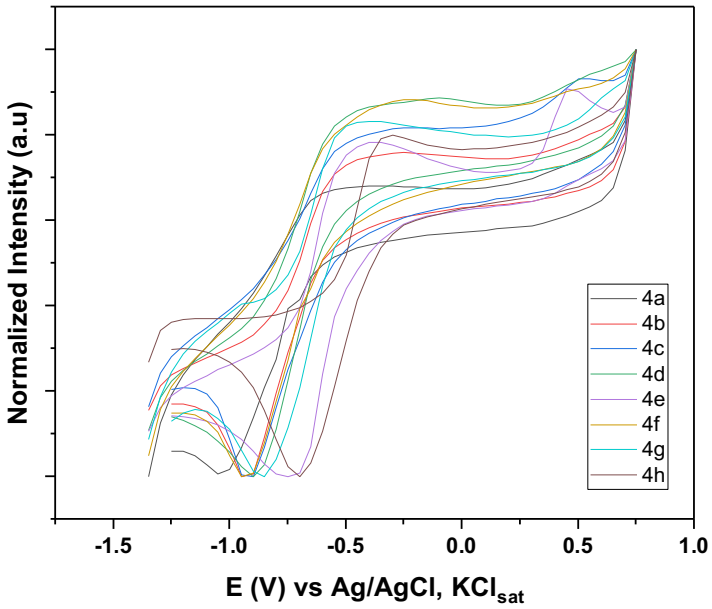

Figure 7: Cyclic voltammetry of acrylohydrazide solutions (c=10^{-3}M) on a platinum electrode, using dimethyl sulfoxide (DMSO) as the solvent, 10^{-1} M sodium chloride (NaCl), and a scan rate of 50 mV/s. The reference electrode used is Ag/AgCl/KCl, with a saturated potential ranging from 1.3V to 0.78V.

The anodic or oxidation potentials of the compounds listed in **Table 7** are uniformly negative and absolute in value, not exceeding 1 V. This observation is rationalized by the presence of the -NH- fragment in the acrylohydrazides. The work by Cauquis et *al*.[17] demonstrated that numerous organic compounds, including aromatic amines, hydrazines, or aromatic nitrogen heterocycles, possessing a lone pair of electrons on a triply bonded nitrogen atom, undergo oxidation below 1 Volt. Our results align with these findings. Comparing the oxidation potential values, compounds **4a**, **4g**, **4b**, **4d**, **4c**, **4e**, **4h**, and **4f** exhibit a trend towards easier oxidation, with lower oxidation potentials indicating increased susceptibility. Consequently,

https://doi.org/10.26434/chemrxiv-2024-f8gtf **ORCID:** https://orcid.org/0000-0003-4573-5978 Content not peer-reviewed by ChemRxiv. **License:** CC BY 4.0

compounds with lower oxidation potentials are expected to be less readily reduced, as reflected by their more negative reduction potentials.

Furthermore, examining the results of cathodic or reduction peak potentials (**Table 7**) reveals consistently negative values. Compounds **4a-e** and **4f-h** are anticipated to pose higher resistance to reduction. The absolute values of the variation between the oxidation peak potential and reduction peak potential (**Table 7**), all exceeding 59 mV, suggest a less reversible process. Cauquis et al.'s studies also emphasized that electrochemical investigations of nitrogen-containing organic compounds remain unaffected by complex phenomena (such as solvent oxidation or electrolyte support oxidation) or the formation of surface platinum oxide films. The conjugation inherent in the acrylohydrazides leads to a general π delocalization effect, stabilizing various intermediates formed during their oxidation. These intermediates are observable through electrochemical methods. The ΔEp values exceeding $\Delta Ep > \frac{59}{n}\ mV$ (assuming a mono-electronic or bi-electronic process with n=1 or n=2, respectively) suggest a quasi-reversible process.

The absolute value of the ratio of anodic to cathodic peak current (**Table 7**) deviates from 1.[18] This deviation indicates a quasi-reversible system, suggesting the possibility of a chemical reaction coupled with charge transfer.

Table 7: Electrochemical data of the studied compounds

Compounds	***Epa (V)***	***Ipa (µA)***	***Epc (V)***	***Ipc (µ A)***	$/\frac{Ipa}{Ipc}/$	***/ΔEp (mV)/***
4a	-0.5731	8.8681	-1.0295	-59.9575	0.14	456.4
4b	-0.4602	8.8737	-0.9380	-57.6428	0.15	477.8
4c	-0.4295	6.6072	-0.9173	-32.1095	0.20	487.8
4d	-0.4602	6.8760	-0.9073	-43.6544	0.15	447.1
4e	-0.3894	14.4284	-0.7549	-64.8075	0.22	365.5
4f	-0.3079	11.1686	-0.9380	-45.2886	0.24	630.1
4g	-.,4753	12.1901	-0.8584	-69.4057	0.17	383.1
4h	-0.3179	11.2507	-0.7041	-52.4448	0.21	386.2

Tableau 8: Energy levels and gap values of the Ox/Red couples of acrylohydrazide derivatives

Compounds	*Peaks*	*Energy level*	*Values (eV)*	*Energie value Gap (eV)*
4a	A_1/A_2	HOMO	-3.09	0.47
		LUMO	-3.56	
4b	B_1/B_2	HOMO	-2.92	0.64
		LUMO	-3.55	
4c	C_1/C_2	HOMO	-3.29	0.38

https://doi.org/10.26434/chemrxiv-2024-f8gtf **ORCID:** https://orcid.org/0000-0003-4573-5978 Content not peer-reviewed by ChemRxiv. **License:** CC BY 4.0

		LUMO	-3.67	
4d	D_1/D_2	HOMO	-3.09	0.61
		LUMO	-3.70	
4e	E_1/E_2	HOMO	-3.14	0.73
		LUMO	-3.87	
4f	F_1/F_2	HOMO	-2.85	0.78
		LUMO	-3.63	
4g	G_1/G_2	HOMO	-3.58	0.20
		LUMO	-3.78	
4h	H_1/H_2	HOMO	-3.56	0.29
		LUMO	-3.85	

The energy levels, as per the Bredas et *al.*[19] empirical relation, are derived from the voltammograms (**Figure S14** in the **ESI**) by plotting tangents and determining the onset oxidation potential (E_{ox}) and onset reduction potential (E_{red}) at their intersections. The HOMO (highest occupied molecular orbital) and LUMO (lowest unoccupied molecular orbital) energies are calculated using the formulas:

$$E_{HUMO} = -(4.4+E_{ref} + E_{ox}) \quad (2)$$

$$E_{LUMO} = -(4.4 +E_{ref +} E_{ox}) \quad (3)$$

with $E_{ref} = 0.20V$ for Ag/AgCl/KCl.

The energy gap ($E_g = E_{HOMO\ (ox)} - E_{LUMO\ (red)}$) estimated from the difference between the onset oxidation and reduction potentials is utilized to determine the separation between the Oxidant and Reductive entities. The calculated energy levels and optical gap values for compounds **4a-h**, obtained from the Bredas et *al.* empirical relation, are presented in **Table 8**. The calculated optical gap values range from 0.09 to 0.31 eV (**Table 8**), indicating that compounds **4a-h** behave as organic semiconductors.

Conclusion

This study successfully synthesized eight new derivatives of (E)3-furan-2-yl acrylohydrazide. The obtained compounds were comprehensively characterized through spectroscopic analyses, including 1D and 2D NMR, as well as high-resolution mass spectrometry.

The ^1H NMR data analysis revealed conformational diversity within the synthesized compounds. Compounds **4a-b** exhibited an Ec=c sp $E_{C=N}$ configuration, whereas compound **4e** displayed an Ec=c ap $E_{C=N}$ configuration. Compounds **4f** and **4h** featured an Ec=c ap $Z_{C=N}$ configuration. UV-visible results demonstrated the compounds' absorption in the visible range. Cyclical voltammetry results indicated the reversible reduction of our acrylohydrazides on a platinum electrode.

https://doi.org/10.26434/chemrxiv-2024-f8gtf **ORCID:** https://orcid.org/0000-0003-4573-5978 Content not peer-reviewed by ChemRxiv. **License:** CC BY 4.0

This study further highlighted the prevalence of specific conformers based on the nature of substituents. UV-visible absorption spectra of N-acylhydrazones confirmed their ability to absorb within the spectral range of 500 to 750 nm. Additionally, cyclical voltammetry results suggested that (E)-3-(furan-2-yl) acrylohydrazide derivatives could undergo oxidation and reduction processes on a platinum electrode, implying intriguing electrochemical properties.

Ultimately, this research contributes to the continuum of prior investigations on N-acylhydrazones, emphasizing the stability of (E)-3-(furan-2-yl) acrylohydrazides. This understanding of their conformation, optoelectronic, and electrochemical properties opens promising avenues for future applications in diverse fields, such as the design of new materials for optoelectronic devices and bioactive compounds.

Conflicts of Interest

There are no conflicts to declare.

Acknowledgments:

We extend our sincere gratitude to the Strategic Support Program for Scientific Research (PASRES, grant number 235, 1st session, 2020) and the Ministry of Higher Education of Côte d'Ivoire for their financial support to P.M.A.C. Special appreciation is also directed towards the University of Paris Cité (France) for providing access to NMR and HRMS spectroscopies. The laboratory of Applied and Fundamental Physical Sciences at Ecole Normale Supérieure deserves our acknowledgment for their assistance with cyclic voltammetry.

In addition, we dedicate this work to Professor Adjou Ané, who unfortunately passed away without having seen the outcome of this work. The untimely occurrence of this departure saddens us all at the time of submitting this article. He provided invaluable guidance throughout the entirety of this research, and his influence will forever resonate in our work.

Authors contributions:

P.M.A.C performed the syntheses, spectral experience and voltammetry. N.S.R gave his assistant for the cyclic voltammetry. P.M.A.C, S.C, A.B.K and A.A participated in the design and direction of the project. D.S, and A.A, supervised the project. P.M.A.C, E.A and S.C wrote the paper. All authors have read and agreed to the published version of the manuscript.

https://doi.org/10.26434/chemrxiv-2024-f8gtf **ORCID:** https://orcid.org/0000-0003-4573-5978 Content not peer-reviewed by ChemRxiv. **License:** CC BY 4.0

References

1. Popiołek, Ł, Patrejko P, Grzywacz G.M., Biernasiuk A., Rycerz-B.A, Chomicka-N.D, Chmiel-P.I, Gumieniczek A., Dudka J., Wujec. M., *Biomed & Pharmacother*. **2020**, 130, 110526

2. Coulibaly S, Evrard A, Kumar A, Sissouma D. *ChemRxiv*. **2023**; doi:10.26434/chemrxiv-2023-trm05-v3

3. Popiołek, Ł. Int. J. Mol. Sci. 2021, 22, 9389.

4. Zheng L.W, Wu L.L, Zhao B.X, Dong W.L, Miao J.Y. *Bioorg Med Chem.* **2009** ;17(5):1957-62.

5. Terzioglu N, Gürsoy A. Eur J Med Chem **2003**; 38: 781–786.

6. Cardoso, L. N., Bispo, M. L., Kaiser, C. R., Wardell, J. L., Wardell, S. M., Lourenço, M. C., & de Souza, M. V. *Arch Pharm*, **2014**, 347(6), 432-448.

7. Umut Salgin-Goksen, Gokcen Telli, Acelya Erikci, Ezgi Dedecengiz, Banu Cahide Tel, F. Betul Kaynak, Kemal Yelekci, Gulberk Ucar, and Nesrin Gokhan-Kelekci, *J Med Chem* **2021**, 64 (4), 1989-2009

8. Yan Z. and Mihail B. *Chem Rev* **2016**, 116 (3), 809-834

9. Ge, Y.Q., Li, F.R., Zhang, Y.J., Bi, Y.S., Cao, X.Q., Duan, G.Y., Wang, J.W. and Liu, Z.L. *Luminescence*, **2014**, 29: 293-300.

10. D. Kitazawa, G. Tominaga, A. Takano, Jpn. Kokai Tokkyo Koho JP 2001057292, *Chem. Abstr.,* **2001**, 134, Article ID: 200276.

Nakamura , H. Yamamoto, PCT Int. Appl. WO 2005043630; *Chem. Abstr.*, **2005**, 142, 440277

11. Patrick-A.A., Siomenan C., Kouassi Y.G. M., Souleymane C., Signo K:, *Synth Commun*, **2022**, 52:9-10, 1306-1317

12. Ablo E, Coulibaly S, Coulibali S, Signo K, Achi PA, Giraud N, Bertho G. *Magn Reson Chem.* **2022**, 60(12):1157-1170.

13. Amer El-Batta, Changchun Jiang, Wen Zhao, Robert Anness, Andrew L. Cooksy, and Mikael Bergdahl. *J. Org. Chem.* **2007**, 72, 14, 5244–5259.

14. G. Palla, G. Predieri, P. Domiano, C. Vignali, W. Turner, *Tetrahedron*, **1986**, 42, 13, 3649-3654

15. Li, K., Xie, R., Zhong, W., Lin, K., Ying, L., Huang, F., Cao, Y,. *Sci. China Chem.* **2018**, 61, 576–583.

https://doi.org/10.26434/chemrxiv-2024-f8gtf **ORCID:** https://orcid.org/0000-0003-4573-5978 Content not peer-reviewed by ChemRxiv. **License:** CC BY 4.0

16. Cauquis, G. *Pure Appl. Chem.* **1971**, 25, 365–378.

17. Diouf, O., Sall, D. G., Gaye, M. L. & Sall, A. S., *C. R. Chim.* **2007**, 10, 473–481.

18. J. L. Bredas, R. Silbey, D. S. Boudreaux, and R. R. Chance, *J. Am. Chem. Soc.,* **1983**, 105, (22), p. 6555-6559.

https://doi.org/10.26434/chemrxiv-2024-f8gtf **ORCID:** https://orcid.org/0000-0003-4573-5978 Content not peer-reviewed by ChemRxiv. **License:** CC BY 4.0